

Progress of a cross-correlation based optical strain measurement technique for detecting radial growth on a rotating disk

Michelle M. Clem and Mark R. Woike

National Aeronautics and Space Administration
Glenn Research Center
Cleveland, Ohio 44135

Ali Abdul-Aziz

Cleveland State University
Cleveland, Ohio 44115

ABSTRACT

The Aeronautical Sciences Project under NASA's Fundamental Aeronautics Program is interested in the development of novel measurement technologies, such as optical surface measurements for the in situ health monitoring of critical constituents of the internal flow path. In situ health monitoring has the potential to detect flaws, i.e. cracks in key components, such as engine turbine disks, before the flaws lead to catastrophic failure. The present study, aims to further validate and develop an optical strain measurement technique to measure the radial growth and strain field of an already cracked disk, mimicking the geometry of a sub-scale turbine engine disk, under loaded conditions in the NASA Glenn Research Center's High Precision Rotordynamics Laboratory. The technique offers potential fault detection by imaging an applied high-contrast random speckle pattern under unloaded and loaded conditions with a CCD camera. Spinning the cracked disk at high speeds (loaded conditions) induces an external load, resulting in a radial growth of the disk of approximately 50.0- μm in the flawed region and hence, a localized strain field. When imaging the cracked disk under static conditions, the disk will be undistorted; however, during rotation the cracked region will grow radially, thus causing the applied particle pattern to be 'shifted'. The resulting particle displacements between the two images is measured using the two-dimensional cross-correlation algorithms implemented in standard Particle Image Velocimetry (PIV) software to track the disk growth, which facilitates calculation of the localized strain field. A random particle distribution is adhered onto the surface of the cracked disk and two bench top experiments are carried out to evaluate the technique's ability to measure the induced particle displacements. The disk is shifted manually using a translation stage equipped with a fine micrometer and a hotplate is used to induce thermal growth of the disk, causing the particles to become shifted. For both experiments, reference and test images are acquired before and after the induced shifts, respectively, and then processed using PIV software. The controlled manual translation of the disk resulted in detection of the particle displacements accurate to $\sim 1.75\%$ of full scale and the thermal expansion experiment resulted in successful detection of the disk's thermal growth as compared to the calculated thermal expansion results. After validation of the technique through the induced shift experiments, the technique is implemented in the Rotordynamics Lab for preliminary assessment in a simulated engine environment. The discussion of the findings and plans for future work to improve upon the results are addressed in the paper.

I. MOTIVATION AND INTRODUCTION

Gas turbine engines operate in severe environmental conditions and are repeatedly exposed to high thermal and mechanical loads. The cumulative effects of these external forces can lead to high stresses and strains on the engine turbine disks. Such strain is a precursor to a fault and can lead to a crack forming in the disk, which could eventually lead to a catastrophic failure. Current fault detection techniques for gas turbine engines are limited to periodic physical inspections and schedule-based maintenance to ensure the integrity of the engine components over the lifetime of the

engine. Unfortunately, these methods have their limitations and failures have been experienced, leading to engine shutdowns and unplanned maintenance. Typically, strain is detected and measured using strain gages, which are a mature and reliable physical measurement technique, however they are intrusive and not easily implemented on an engine turbine disk as transmitting signals to and from the strain gages can become cumbersome. Furthermore, strain gages provide point measurements, therefore requiring numerous gage installations and interpolation in between points in order to obtain a global strain field. Currently, non-intrusive measurement techniques available to measure the strains experienced by the turbine engine disk do not exist. Therefore, in an effort to prevent future failures caused by undetected strains and faults in the gas turbine engines and their components, the development of fault detection techniques in the form of new sensor technologies or methods for in situ structural health monitoring is of high interest to NASA. Presently, external sensors are under development at NASA Glenn Research Center's (GRC) High Precision Rotordynamics Laboratory including Microwave Blade Tip Clearance (MBTC)¹⁻³ sensors and Capacitive Blade Tip Clearance (CBTC) sensors⁴. Although these techniques would be non-intrusive to the turbine engine disks, they still require hard mounting through the engine casing. Alternatively, optical techniques are also being pursued as potential non-intrusive strain measurement techniques. These techniques include the implementation of a Moiré Pattern⁵ as well as a potential cross-correlation based technique using an applied particle pattern⁶. The current study expands upon the initial development of the cross-correlation based optical strain measurement technique⁶ and is being pursued by the Innovative Measurements Task within the Aeronautical Sciences Project under NASA's Fundamental Aeronautics Program, to develop optical surface measurements for internal flow diagnostics.

The present optical measurement technique offers potential strain and fault detection by measuring the radial growth, of a pre-cracked disk, mimicking the geometry of a sub-scale engine turbine disk, operating under loaded conditions in the Rotordynamics Laboratory. The cross-correlation based technique consists of imaging a high-contrast random particle pattern that is applied to an area of interest on a disk. Due to the induced fault (machined crack), the disk experiences a concentrated amount of radial growth surrounding the crack, while operating under loaded conditions (i.e. rotating at speeds up to 15,000 rpm). The radial growth results in the pattern being shifted, therefore creating a displacement of the particle pattern. Images are acquired of the pattern before and after the loading and the resulting particle displacements are measured using 2D cross-correlation algorithms of Particle Image Velocimetry (PIV) software. Using PIV optimization guidelines, a previous study⁶ was performed to develop an effective pattern for detecting the expected radial growth (i.e. the particle displacements). The optimal pattern design was found to be one consisting of retro reflective micro-glass beads ranging from 40- μm - 100- μm in diameter. The micro-glass bead pattern was adhered onto a thin aluminum plate and was found to effectively detect both manually and artificially induced 50.0- μm shifts, which is the expected maximum radial growth of the disk⁶. The current study continues the development of this technique by applying the optimal pattern directly onto the surface of the disk and carrying out two benchtop experiments to further investigate the technique's effectiveness at detecting the expected particle displacements. The applied particle pattern is first displaced through manual translation and secondly through thermal expansion. After validation in the benchtop experiments, the disk is transferred to the Rotordynamics Laboratory to analyze the technique in a simulated engine environment where preliminary data is acquired.

Continued development and refinement of the optical strain measurement technique may lead to the ability of providing global strain and growth mapping for potential in situ health monitoring of engine turbine disks. In addition, due to the technique's minimal setup, it has potential for use outside of the engine environment as well as laboratory strain diagnostic work for both static and rotating objects.

II. THEORY

In the current study, cross-correlation algorithms are used to calculate the particle pattern displacements between the reference image of the static disk and the image of the rotating disk under loaded conditions. During rotation the cracked region will grow radially, thus causing the applied pattern to shift, resulting in a pattern (image) displacement, relative to the image of the unloaded disk. The pattern applied to the disk consists of a high-contrast random particle pattern. Due to radial growth of the cracked disk under loaded conditions, the particles move a finite distance between the two images, therefore making cross-correlation based PIV algorithms a good choice to calculate the particle displacement. Due to the fact that PIV algorithms are used to determine the resulting image displacements, the optimization principles of PIV drive the design and evaluation of the particle pattern being used in the optical strain measurement technique.

A schematic of a typical setup for the optical strain measurement technique is shown in Fig. 1(a). An incoherent light source illuminates the random particle pattern. A camera and lens system placed at distance, Z_o , away images the particle positions onto the image plane. A reference image of the pattern is acquired in its static position. Due to an induced shift or external load, the particle pattern experiences a displacement, indicated by the overlapping dashed pattern figure, and a second image is acquired. The particle displacements from the two images are processed by dividing the image up into small interrogation windows (sub-regions) and cross-correlating the corresponding sub-regions. The sub-region from image one is cross-correlated via FFT operations with the same sub-region from image two. The location of the displacement peak from the origin on the correlation plane gives the displacement vector magnitude and direction. This process is illustrated in Fig. 1(b) (acquired from [7] and is repeated over the entire image plane resulting in spatially averaged displacement vectors.

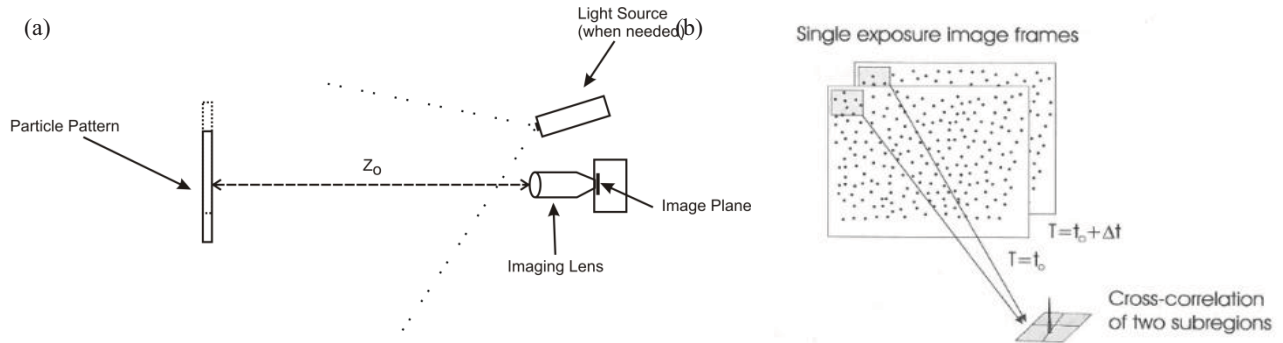


Figure 1. (a) Schematic of a typical setup for the optical strain measurement technique and (b) illustration of the sub-region cross-correlation process that is repeated over the entire image resulting in spatially averaged displacement vectors [7].

Successful cross-correlation of the sub-regions across the entire image depends on the ability to identify the displacement correlation peak, with respect to the random correlation noise. An optimal correlation peak signal to noise ratio can be found when the number of particles per sub-region is nominally 10. The accuracy of the displacement estimates (i.e. correlation peak position error) determined from the sub-region cross-correlations is primarily determined by the ratio of the effective particle diameter and the sub-region size. Note, in order to avoid aliasing in the correlation plane, the displacement should be less than $1/4^{\text{th}}$ of the sub-region size. It has been found that by using interpolation techniques, the correlation peak position error can be determined to sub-pixel accuracy; nominal values for the error are on the order of 0.1-pixel for particles spanning 1-2 pixels⁸⁻¹¹.

In summary, the guidelines being employed in the development and evaluation of the pattern being used in the optical strain measurement technique are:

1. There are nominally 10 particles per sub-region
2. The imaged particle (effective particle diameter) spans 1-2 pixels
3. The sub-region is chosen, such that maximum displacement is less than $1/4^{\text{th}}$ of the sub-region size

These guidelines were previously discussed in⁶ and more detailed reviews and discussions of the fundamentals and optimization principles of Digital Particle Image Velocimetry (DPIV) can be found in [12-13].

III. EXPERIMENTAL SETUP AND PROCEDURE

A. Manual translation and thermal expansion experiments for the optical technique development and validation

Two benchtop experiments are performed to further validate the optical strain measurement technique under investigation. The optimized pattern, selected from the previous pattern optimization study⁶, is adhered onto the face of a scaled-engine turbine-like disk; the pattern consists of 40- μm - 100- μm glass beads applied over the entire surface using a spray adhesive with an approximate concentration of 39 particles/ mm^2 . The 32-blade disk is 12.7-mm thick, 190-mm in diameter (not including the length of the blades), and is composed of Aluminum 6061 - T6. Figures 2(a) and

2(b) show the aluminum disk before and after the pattern is applied to the surface, respectively. Note, a notch 50.8-mm in length (indicated in Fig. 2(b) by the yellow circle) was machined into the disk in order to simulate a crack/fault to expedite deformation (i.e. radial growth of the disk) while operating under loaded conditions.

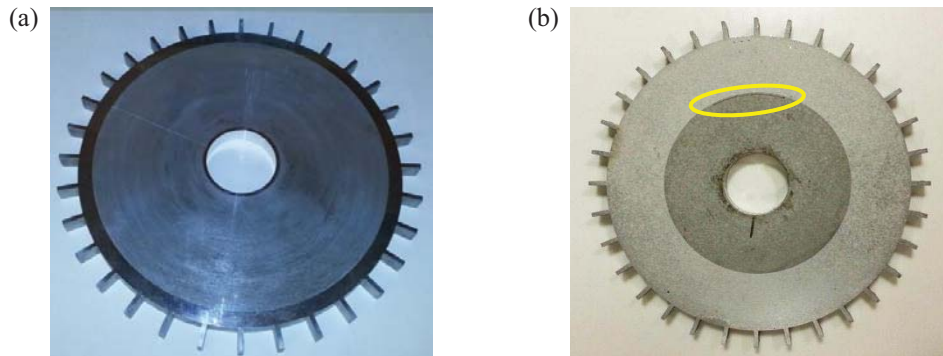


Figure 2. (a) Image of the 32-blade, 12.7-mm thick, 190-mm in diameter (not including the blades), disk composed of Aluminum 6061 – T6 used in the present study and (b) image of the same disk with the micro-glass bead pattern adhered on the front surface and a crack machined into the disk (circled in yellow).

The disk is first mounted onto a translation mechanism equipped with a fine micrometer and a manual shift (i.e. particle displacement) is applied perpendicular to the optical axis. A 50- μm shift was chosen in order to replicate the expected maximum growth of the flawed turbine disk while operating under loaded conditions in the Rotordynamics Laboratory⁶. A Princeton Instruments EC11000 scientific-grade CCD camera is mounted looking into the plane of the disk and the applied pattern is imaged onto the camera's 4008 pixels x 2672 pixels detector using a 60-mm lens. The imaging system is setup to image only the cracked region of the disk to enable increased resolution over the area of interest. Reference and data images were acquired of the applied pattern before and after the induced particle displacements. After verification of the manual particle displacements, the translation mechanism was replaced with a hotplate in order to induce a particle shift due to thermal expansion (i.e. thermal growth). The back surface of the disk was placed flatly onto the top surface of the hotplate to enable uniform heating. A type K thermocouple is adhered onto the side of the disk's cracked region in order to acquire reference temperature measurements. Figure 3 depicts an image of the setup used for both the manual translation and thermal expansion experiments. Note, the imaging system setup remained the same for both experiments; only the manual translation stage and hotplate were interchanged for the manual translation and thermal growth experiments, respectively.



Figure 3. Setup used for both the manual translation and thermal expansion experiments. The imaging system remained the same for both experiments and only the manual translation stage and hotplate were interchanged with one another for the manual translation and thermal growth experiments, respectively.

Due to the different heights of the translation stage and hotplate, the resulting fields of view and scale factors are slightly different; the scale factor for the manual translation experiment is 38.1 pixels/mm and the scale factor is 54.7 pixels/mm for the thermal expansion experiment. The image pairs were processed using the cross-correlation algorithms available in PIV software. Ten pairs of image pairs were processed for the manual translation experiment whereas one pair of images was acquired at a time for the thermal expansion study. An image was acquired at the ambient room temperature of 20°C and the test image was acquired when the disk had settled out at 100°C.

B. Implementation of the optical technique in the High Precision Rotordynamics Laboratory

After completion of the benchtop validation experiments, the disk was then implemented in the Rotordynamics Laboratory at NASA GRC for preliminary evaluation of the technique's ability to detect the radial growth of the cracked disk while operating under loaded conditions. The Rotordynamics Lab consists of a spin rig which is capable of simulating engine environments for engine rotor disks up to 254-mm in diameter. The rig has a stainless steel shaft with a length of 781-mm and diameter of 20-mm, which is supported by precision contact ball bearings on each end and has adjustable dampers. An encoder is mounted on the end of the shaft which is used by the control system to provide closed-loop control of rig speed and a secondary optical tachometer (once per rev signal) is used to record the speed into the data system and to synchronize the data to the rig's rotation. A 12-hp custom-built, direct-current (dc) motor is used to rotate the spin rig and the simulated engine disks up to speeds of 15,000 rpm. Figure 4 shows the disk with the applied pattern successfully installed onto the spin rig. Note, annotations of the rig's key components are included.

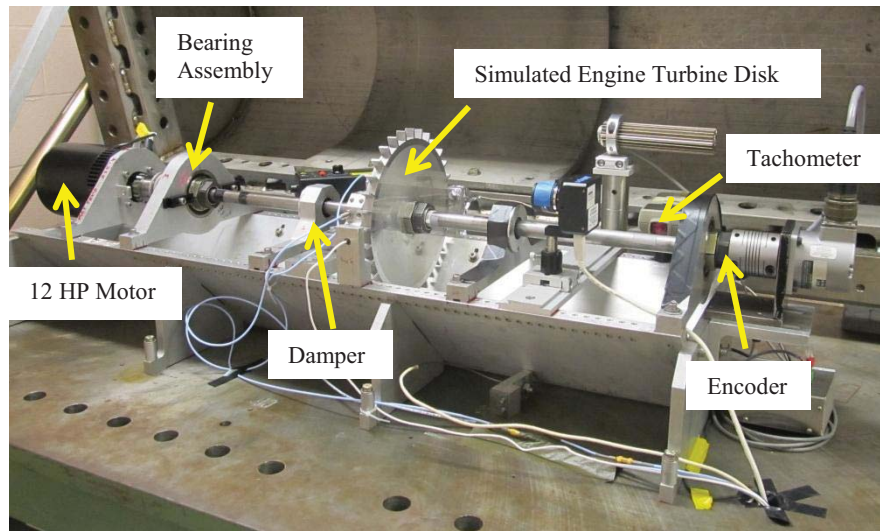


Figure 4. The High Precision Rotordynamics Lab at NASA GRC in which the optical technique is implemented to evaluate the technique's ability to detect the radial growth of the cracked disk while operating under loaded conditions.

Due to equipment failure, a Mightex camera equipped with a 25mm lens was used to image the cracked region of the disk onto a 2592x1944 detector in place of the previously used Princeton Instruments camera. The resulting scale factor is approximately 43.8 pixels/mm, which is similar to the scale factors used in the bench-top experiments.

IV. RESULTS AND DISCUSSION

A. Manual translation and thermal expansion experiments for the optical technique development and validation

In order to further develop and validate the optical strain measurement technique two benchtop experiments inducing particle shifts are performed. As previously stated, the optimal pattern is adhered onto the turbine-like disk. To apply the pattern, the micro-glass beads are scattered onto the disk and adhered using a spray adhesive. Once applied, it was necessary to verify that the pattern still meets the PIV optimization guidelines discussed in Section II: the particle

diameter should span approximately 1-2 pixels, there should be nominally 10 particles per sub-region, and the particle displacement should be less than $1/4^{\text{th}}$ of the sub-region size.

In order to avoid aliasing in the correlation plane, the particle displacement should be less than $1/4^{\text{th}}$ of the sub-region size. It is known from prior computational analysis⁶ that the largest expected radial shift to occur on the proposed cracked disk is approximately 50.0- μm at 15,000 rpm. Using the scale factor, a shift of 50.0- μm corresponds to a pixel shift in the image plane of approximately 2.73 pixels. Therefore, the sub-region size in the present study was set to 16 x 16 pixels, thus meeting the PIV optimization criteria. The smallest sub-region size that met this criteria was chosen in order to provide the finest spatial resolution possible.

A representative 16 x 16 pixel sub-region, depicted by the yellow square, from an image of the micro-glass bead pattern adhered onto the disk is shown in Fig. 5. Due to the difficulty of controlling the density of the micro-glass beads during application, the particle density varies across the sub-regions throughout the image. Therefore, Fig. 5 depicts an “average” sub-region consisting of a region that is neither the densest nor the least dense. It is verified in the image that the effective diameter of the glass beads when imaged through the optical system spans 1-2 pixels and approximately 6-7 particles appear in one sub-region instead of the optimal number of nominally 10 particles per sub-region. However, it is important to note that having a lesser or greater number of particles does not decrease or increase the accuracy of the correlation peak position; instead having the optimal number of particles per sub-region increases the probability that the correlation peak of the two sub-regions will be larger than the random noise in the spatial correlation, therefore increasing the likelihood of correctly identifying the correlation peak.

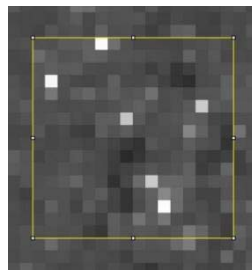


Figure 5. A zoomed in view of a representative 16 x 16 pixel sub-region window showing the particle density and the effective particle diameter size (in pixels) for the micro-glass bead pattern adhered onto the surface of the turbine-like disk.

A manual translation experiment was performed to ensure the applied pattern was sufficient in accuracy at detecting the disk’s expected maximum radial growth of 50.0- μm . Note, the experiments concentrate on investigating the flawed region. Figure 6 shows a sample image acquired of the disk during the manual translation experiment; only the cracked region is imaged by the camera and lens system in order to increase spatial resolution across the area of interest.



Figure 6. A sample image acquired of the disk during the manual translation experiment.

The pattern was manually shifted 50.0- μm in the horizontal direction (perpendicular to the optical axis) using the micrometer setup previously described. Note the pattern was not shifted in the vertical direction; therefore the known vertical shift is 0.0- μm , assuming the translation stage is perfectly aligned perpendicular to optical axis of the imaging system. A total of 10 reference and data image pairs were processed using a 16x16 pixel sub-region that was translated across each of the entire images to produce spatially averaged displacement vectors. Since the patterns were shifted as a whole in the horizontal direction, ideally every point on the pattern moved the same distance. Therefore, a total of 1,673,340 spatially averaged displacement vectors resulting from the cross-correlation routine for all 10 image pairs were averaged to produce an overall particle displacement vector, referred to as the “detected shift”. Table 1 summarizes the detected shifts and their standard deviation compared to the known shifts for both the horizontal and vertical directions for the micro-glass bead particle pattern applied to the surface of the disk.

Table 1: Summary of the detected shifts for each particle pattern compared to the known shift in both the horizontal and vertical directions.

Known Horizontal Shift (μm)	40 – 100 μm Glass Beads Detected Horizontal Shift (μm)	Known Vertical Shift (μm)	40 – 100 μm Glass Beads Detected Vertical Shift (μm)
50.0	49.66 ± 1.88	0.0	0.48 ± 0.68

The accuracy of the displacement vectors is primarily determined by the ratio of the correlation peak size to the sub-region size. Nominal values for the peak positioning error are on the order of 0.1-pixel (approximately 2.60- μm using the manual translation scale factor) for particles spanning 1-2 pixels. It is evident in Table 1 that standard deviations associated with the detected shifts for both directions fall below the nominal range of error. The average error leads to correlation peak estimates that are accurate to $\sim 1.75\%$ of full scale; optimal PIV setup leads to velocity estimates accurate to nominally 1% of full scale⁹. Note, the error for the horizontal shifts is higher than that of the vertical shifts; it is suspected that the higher horizontal error is due to the patterns being manually shifted 10 times in the horizontal direction via the translation stage, consequently introducing manual human positioning errors. The bias error in the mean detected shift values is most likely a result of the positioning errors. The patterns were not manually shifted in the vertical direction and therefore should have less error, as seen in the data; in fact, all of the detected vertical shift error is below the nominal expected range of error. These results follow the same trend reported in⁶ and verify that the newly applied micro-glass bead pattern has the ability to accurately detect the expected radial growth of the disk under loaded conditions.

To further validate the present optical strain measurement technique, a thermal expansion experiment was performed using a hotplate to induce thermal growth of the disk, thus causing the pattern on the disk to become displaced. The disk was placed flat onto the hotplate. Reference and test images were recorded when the thermocouple settled out at 20 °C and 100 °C, respectively. A sample reference image is shown in Fig. 7. Again, the imaging system was setup such that the cracked region was in the field of view.

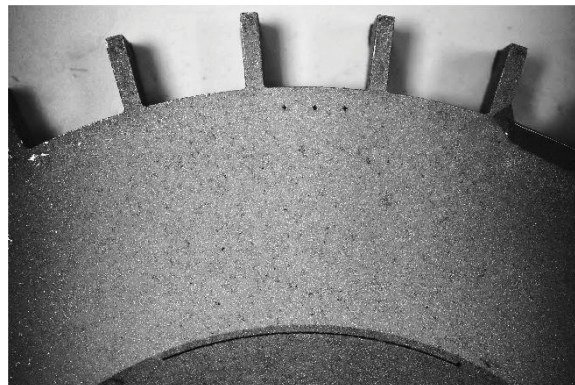


Figure 7. Sample reference image acquired during the thermal expansion experiment. The imaging system was configured so that the cracked region of the disk comprises the field of view.

It was attempted to obtain a physical reference measurement of the thermal growth to compare to the value obtained from the present optical technique, however, acquiring a reference measurement with high enough precision proved to be very challenging. Several methods were attempted, but none resulted in reliable and repeatable reference measurements; therefore, a thermocouple was used to attain temperature measurements in order to calculate the theoretical value of the disk's thermal growth, assuming linear expansion, for comparison to the optical technique. Equation 5 expresses the linear thermal expansion, ΔL , where α is the coefficient of thermal expansion, ΔT is the change in temperature, and L is the disk's radius¹⁵. Because the disk is expected to grow in the radial direction, a factor of $\sqrt{2}$ is added to the equation, to better represent the thermal growth (assuming the disk grows equally in both the x and y directions). Being that the disk is composed of Aluminum 6061-T6, $23.6 \mu\text{m}/\text{m}^\circ\text{C}$ (average over the range of 20-100°C) is substituted in for the thermal expansion coefficient.

$$\Delta L = \sqrt{2}\alpha\Delta TL \tag{5}$$

The image pairs are processed using the PIV correlation algorithms and the particle displacements are plotted as contours to better visualize the thermal growth results. Figure 8 depicts a sample plot of the thermal growth of the disk. The legend represents the magnitude of the particle displacements and the units are given in pixels. The physical thermal growth values are subsequently determined using the appropriate scale factor. The results shown in Fig. 8 follow the expected trend: the disk appears to expand radially outward with the most thermal growth occurring at the outer radius and blades. However, the growth appears to be growing non-uniformly across the disk, which is most likely occurring due to the temperature across the disk being non-uniform.

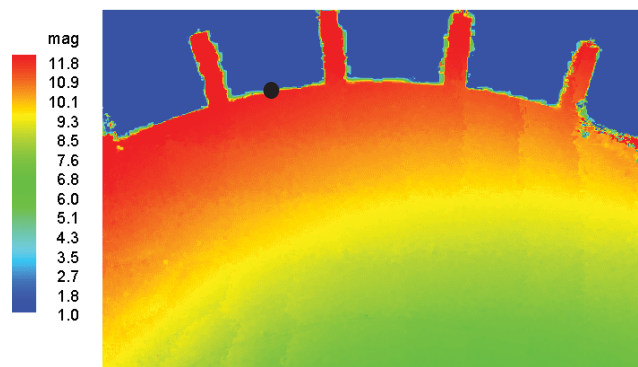


Figure 8. Sample contour plot of the calculated particle displacements caused from the linear thermal expansion of the disk. The legend represents the magnitude of the particle displacements and are given in units of pixels. Physical thermal growth values are determined using the appropriate scale factor. The black dot represents a sample location of the calculated thermal growth.

The thermal growth is estimated at a sample location (indicated by the black dot in Fig. 8) along the disk's outer radius (not including the blade length). Substituting the radius of 95-mm for L and 80°C for ΔT into Eq. 5, the theoretical thermal growth in the radial direction at the indicated point is estimated to be $253.4\text{-}\mu\text{m}$. The particle displacement value, corresponding to the thermal growth measurement of the disk, was found to be $268.9\text{-}\mu\text{m} \pm 2.28\text{-}\mu\text{m}$ (using the scale factor to convert). Note, the error is estimated using the nominal value of 0.1-pixel for the peak positioning error since the imaged particles were previously shown to span approximately 1-2 pixels. The estimated thermal growth measured by the optical technique agrees reasonably well with the theoretical value.

B. Implementation of the optical technique into the High Precision Rotordynamics Laboratory

After completion of the benchtop validation experiments, the disk was then implemented into the Rotordynamics Laboratory to investigate whether or not the technique can detect radial growth of the cracked disk while operating under loaded conditions. The disk was successfully installed onto the spin rig. A pulsed LED was used to “freeze” the motion of the rotating disk. It was attempted to use a pulse delay circuitry to rotate the cracked region of the disk into the desired field of view, however it was not as stable as desired resulting in a blurred image of the disk. Therefore, in an

effort to obtain a more crisp image of the disk and to rotate the region of interest into the field of view, the once per rev signal was adjusted manually. When moving the once per rev signal it was necessary to first move the signal and then run the rig to determine whether or not the desired region was within the field of view. Once the cracked region was in the field of view, the rotational speed was increased to see if the imaged region would remain steady (the desired region would shift out of view due to slipping of the disk on the shaft while under rotation). During the process of checking out the once per rev signal and the resulting field of view, the disk was brought up and down from rotational speed multiple times. Upon successfully reaching a steady image of the cracked region, the disk was brought up and held temporarily at 10,000 rpm and then increased and held at 12,000 rpm for check-out purposes and preliminary data were acquired at both loaded conditions. Figure 9 shows a resulting image acquired at 10,000 rpm after moving the once per rev signal; the cracked region appears stationary in the field of view. The image obtained from moving the once rev per signal is much more clear and crisp than the image obtained using the pulse delay circuitry, however an image from the pulse delay circuitry was not acquired and therefore not available for comparison. Note, three small crosshairs (circled in yellow) were laser etched onto the disk's outer diameter and a dot was manually applied to the disk's inner diameter (circled in green) for image registration purposes. Registering the unloaded versus loaded images, before processing the image pair via correlation algorithms, would help to decrease any bias error/shift that may have occurred other than radial growth (i.e. shifting of the disk on the spin rig).

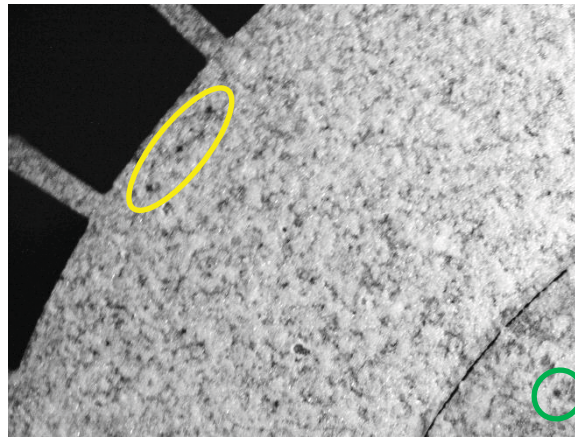


Figure 9. Sample image of disk acquired at 10,000 rpm. The motion of the disk was “frozen” using a pulsed LED. Manually adjusting the once per rev signal moved the cracked region into the field-of-view. after moving the once per rev signal; the cracked region appears stationary in the field of view. The yellow and green circles indicate registration marks.

After acquiring data at 10,000 and 12,000 rpm, the disk was brought back to unloaded (0 rpm) conditions to acquire static reference images. It was intended to acquire reference images and then repeat the data acquisition at loaded conditions (now that the once per rev signal was set). However, when inspecting the static disk it was discovered that the micro-glass bead pattern had not retained its adhesion onto the disk and had partially disintegrated. Moreover, the pattern appeared to be most disintegrated in the cracked region of the disk, offering physical evidence that the disk is growing radially under loaded conditions due to the induced fault. It is suspected that the radial growth is weakening the adhesive bonds between the particles and the disk's surface, thus causing the particles to come off of the disk while rotating. Figures 10(a)-10(b) show images of the deteriorated pattern, without and with, use of a camera flash (for visualization purposes) after rotating at 10,000 and 12,000 rpm. The crack is outlined by the yellow circle in both images.

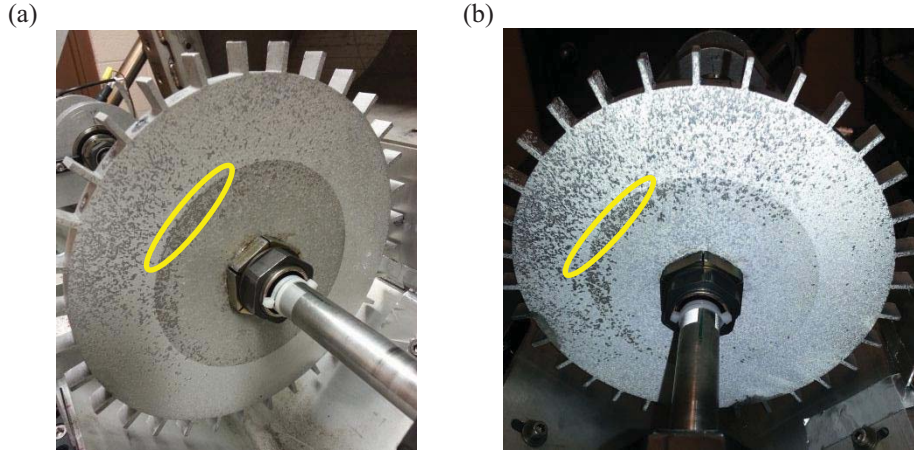


Figure 10. Images of the deteriorated pattern after rotating at 10,000 and 12,000 rpm acquired (a) without a flash and (b) with the flash on. Note, the pattern is much more disintegrated surrounding the region of the crack, suggesting physical evidence that the disk is growing while operating under loaded conditions.

Due to the disintegrated pattern (and time constraints) it was no longer feasible to obtain a reference image of the disk, thus limiting further evaluation of the technique's implementation on the rotating disk. Future work will include investigation of new methods for pattern adhesion to prevent the pattern from deteriorating while rotating at high speeds as well as considering ways to improve the pulse delay circuitry in order to eliminate the need to manually adjust the once per rev signal to obtain a crisp test image. Remotely controlling the once per rev signal would decrease the number of times the spin rig is brought up to high speeds and then down to static conditions, thus prolonging the life of the applied pattern. In addition, image registration methods will also be studied as a tool to adjust for any sources of experimental error, beyond the cross-correlation peak estimation error, resulting in more accurate estimates of the disk's radial growth.

V. CONCLUSIONS AND FUTURE WORK

The present study aims to further develop an optical strain measurement technique first explored in [1] for potential use as a non-intrusive in situ health monitoring technique of gas turbine engines. The basis of the optical strain measurement technique consists of measuring a shift of a high-contrast random particle pattern by imaging the illuminated particles with a CCD camera and using the cross-correlation algorithms in PIV software to evaluate the particle displacements across the area of interest. This paper investigates the effectiveness of the technique to determine the particle displacements of an optimal pattern previously determined in [1] when applied onto a disk, mimicking the geometry of a sub-scale engine turbine disk. Two benchtop experiments were performed to induce shifts onto the disk (i.e. create particle displacements) in order to further validate the technique: the disk was shifted manually using a translation stage equipped with a fine micrometer and thermal growth was induced onto the disk using a hotplate to increase the temperature of the disk to 100°C. For both experiments, reference and test images were acquired before and after the induced shift, respectively, and then processed using the PIV software. The results of the manually induced shift experiment verified that the pattern applied to the disk had the ability to detect the maximum expected radial growth of 50- μm accurate to $\sim 1.75\%$ of full scale. The thermal expansion experiment was deemed successful as the optical technique agreed well with the theoretically calculated thermal growth measurements.

After validation of the optical strain measurement technique through the two benchtop experiments, the technique was tested in NASA GRC's High Precision Rotordynamics Laboratory. The disk (with the applied pattern) was installed on the spin rig and the imaging system was setup accordingly. The disk was spun at 10,000 and 12,000 rpm and a once per rev signal was used to "freeze" the motion of the disk to facilitate the acquisition of test images. Once bringing the disk back down to static conditions, it was realized that the micro-glass bead pattern had disintegrated, especially in the region surrounding the crack, thereby limiting the evaluation of the technique's implementation into the spin rig. Reference images were unable to be acquired due to the deteriorated pattern and therefore preliminary particle displacement results were unable to be calculated. Near term future work will include investigation of new methods of

pattern application as well as improvement of the pulse delay circuitry in order to remove the need to manually adjust the once per rev signal, thus prolonging the life of the applied pattern. Image registration techniques will also be explored as tool to aid in the removal of any sources of experimental error, beyond the cross-correlation peak estimation error, resulting in more accurate estimates of the disk's radial growth. Additional future goals involve mapping the entire strain field experienced by the cracked disk under loaded conditions. Knowing the total deformation (radial growth of the disk) and the original radius of the disk enables calculation of the strain. It should be possible to map out the strain field over the entire circumference of the disk by capturing several images at various points in the disk's rotation cycle. This work has been carried out for the development of potential optical surface measurements for the in situ health monitoring of internal flow parts, such as the engine turbine disk, and are supported by the Innovative Measurements Task within the Aeronautical Sciences Project under NASA's Fundamental Aeronautics Program.

ACKNOWLEDGEMENTS

This work was supported by the Aeronautical Sciences Project under NASA's Fundamental Aeronautics Program. In addition, the author would like to acknowledge Dr. Mark Wernet for use of his PIV software package.

REFERENCES

- [1] Clem, M.M., Woike, M.R., and Abdul-Aziz, A., "Investigation of a cross-correlation based optical strain measurement technique for detecting radial growth on a rotating disk," SPIE Vol. 8693, 86930O-1, 2013.
- [2] Woike, M., Abdul-Aziz, A., Bencic, T., "A Microwave Blade Tip Clearance Sensor for Propulsion Health Monitoring," NASA/TM—2010-216736, AIAA-2010-3308, 2010.
- [3] Woike, M., Abdul-Aziz, "Crack Detection Experiments on Simulated Engine Turbine Disks at NASA Glenn Research Center's Rotordynamics Laboratory," NASA/TM—2010-216239, AIAA-2010-587, 2010.
- [4] Woike, M., Roeder, J., Hughes, C., and Bencic, T., "Testing of a Microwave Blade Tip Clearance Sensor at the NASA Glenn Research Center," NASA/TM—2009-215589, AIAA-2009-1452, 2009.
- [5] Abdul-Aziz, A., Woike, M., Oza, N., Matthews, B., and Baaklini G., "Propulsion Health Monitoring of a Turbine Engine Disk Using Spin Test Data," NASA/TM—2010-216743, 2010.
- [6] Woike, M., Abdul-Aziz, A., Fralick, G., and Wrbanek, J., "Investigation of a Moiré Based Crack Detection Technique for Propulsion Health Monitoring," NASA/TM – 2012-217622, SPIE, 2012.
- [7] Wernet, M., "Fuzzy Logic Enhanced Digital PIV Processing Software," NASA/TM-1999-209274, 1999.
- [8] Wernet, M., Pline, A., "Particle Placement Tracking Technique and Cramer Rao Lower Bound Error in Centroid Estimates in from CCD Imagery," Experiments in Fluids, Vol. 15, No. 4-5, pp.295-307, 1993.
- [9] Adrian, R. J., "Multi-Point Optical Measurements of Simultaneous Vectors in Unsteady Flow-A Review," Int. J. of Heat and Fluid Flow, Vol. 7, pp. 127-145, 1986.
- [10] Westerweel, J., "Fundamentals of Digital Particle Image Velocimetry," Meas. Sci. Technol., Vol. 8, pp. 1379-1392, 1997.
- [11] Westerweel, J., "Theoretical analysis of the measurement precision in particle image velocimetry," Experiments in Fluids, [Suppl], pp. S3-S12, 2000.
- [12] Keane, R., Adrian, R., "Theory of cross-correlation analysis of PIV images," Applied Scientific Research, Vol. 49, pp.191-215, 1992.
- [13] Mercer, C., [Optical Metrology for Fluids, Combustion, and Solids], Kluwer Academic Publishers, Boston, pp. 69-104, (2003).
- [14] Raffel, M., Willert, C., Kompenhans, J., [Particle Image Velocimetry], Springer, Verlag Berlin Heidelberg New York, (1998).
- [15] Young, Hough, D., [Fundamentals of Mechanics and Heat], McGraw-Hill Book Company, United States, pp. 515-518, (1974).